Supporting Information

Small Energy Gap Revealed in $CrBr_3$ by Scanning Tunneling Spectroscopy

Dinesh Baral, Zhuangen Fu, Andrei S. Zadorozhnyi, Rabindra Dulal, Aaron Wang, Narendra Shrestha, Uppalaiah Erugu, Jinke Tang, Yuri Dahnovsky, Jifa Tian, and TeYu Chien*

Department of Physics & Astronomy, University of Wyoming, Laramie, WY 82071

*corresponding author: tchien@uwyo.edu

S1. Energy-dispersive X-ray spectroscopy study on $CrBr_3$.

Figure S1 shows the EDS spectrum (taken at the location indicated by the black dot in the inset SEM image) and the inset scanning electron microscope (SEM) image is of an exfoliated $CrBr_3$ flake on Si/SiO_2 wafer. This result is obtained using FEI QUANTA 450 FEG SEM. As expected, layered texture of the materials is revealed in the SEM image and the Cr:Br ratio is determined to be 1:3 and no other elements are present.

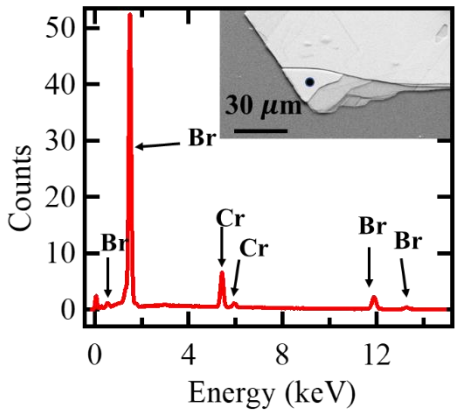

Figure S1: The EDS spectrum taken from a single spot on the sample marked by a black dot shown in inset. The corresponding peaks are identified to be Cr and Br with a molar ratio of 1:3. Inset: SEM image of $CrBr_3$.

S2. Atomic structure of Highly Oriented Pyrolytic Graphite (HOPG) by Scanning Tunneling Microscope (STM) study.

Figure S2(c) shows the atomic resolution image of HOPG measured from STM study near the $CrBr_3$ flakes in ultra-high vacuum (UHV). This image is compared with the crystal structure of the bilayer HOPG, Fig. S2(a) and (b). The lattice constant of HOPG is extracted and consistent with reported value ($a = b = 2.46$ Å). This data indicates that the tip is in good condition prior to the scanning on $CrBr_3$ region as shown in the main text. The distinct atomic resolution images on HOPG and on $CrBr_3$ also provide a direct way of identifying the $CrBr_3$ measurements. In addition, Fig. S2(d) shows the gapless dI/dV spectrum, further confirming the quality of the tip and the distinguishing results from $CrBr_3$.

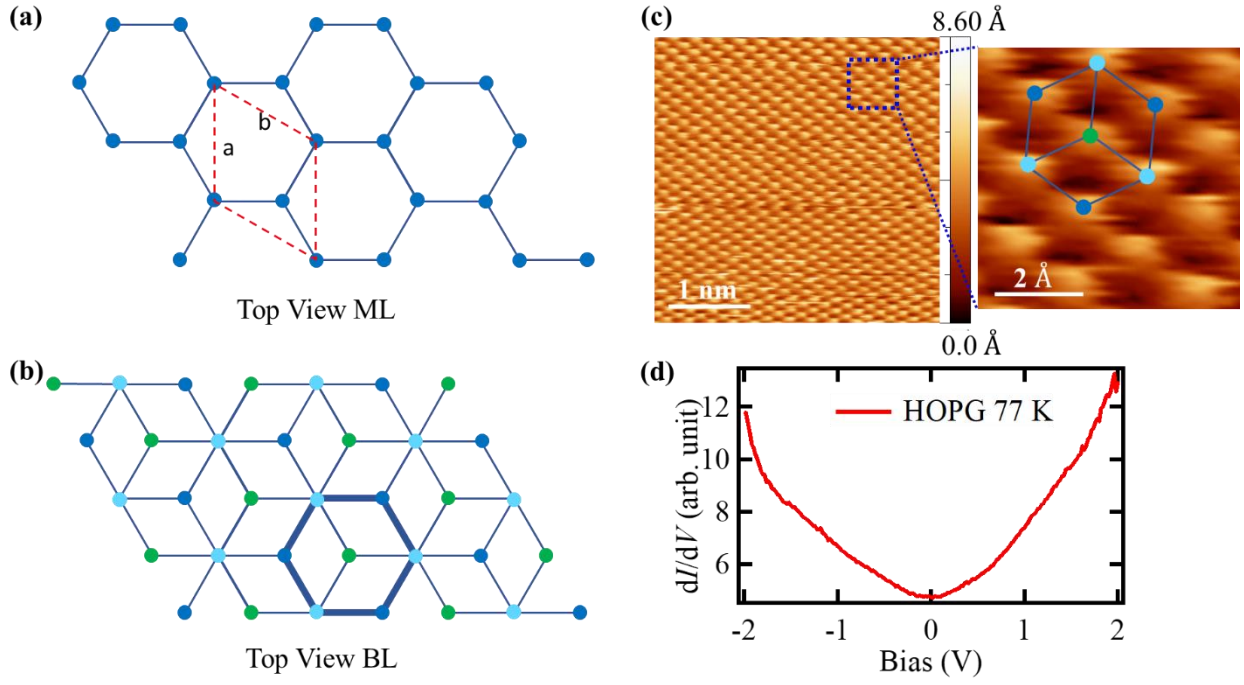

Figure S2. STM study of HOPG: (a) and (b) Structure of monolayer (ML) and bilayer (BL) HOPG respectively. In the bilayer case, blue circles represent C-atom on the top layer, green circles represent C-atom at the bottom layer and the sky-blue circles represent C-atoms appeared at both layers. **(c)** Atomic resolution image of HOPG substrate (Bias: 1 V, set point current: 1 nA). The zoom-in view of the topography is shown to the right with the atomic structure on top. **(d)** dI/dV spectra taken on HOPG at bias ranging from 2 V to -2 V.

While performing STM measurements, we occasionally encountered big chunks of clusters where we cannot get the atomic resolution images. During the measurements, we simply search for clean regions where we could obtain the atomic resolution images on the $CrBr_3$ flakes. The atomic resolution images indicates that our measurements are performed on clean $CrBr_3$ regions and the properties measured are related to the pristine $CrBr_3$.

S3. Multiple peaks featured d*I*/d*V* spectra of $CrBr_3$.

d*I*/d*V* spectra taken at T = 77 K with lock-in amplifier at different bias range ($\pm$ 0.8 V, $\pm$ 1 V, $\pm$ 2 V and $\pm$ 3 V) and sensitivity setting are shown in Fig. S3(a). Multiple-peak features are further confirmed with derivative of the measured *I*-*V* curve, which shows that all the measured d*I*/d*V* curves are consistent with the derivative of the *I*-*V* curve. To show the consistency we present the comparison for the case of the bias range of $\pm$ 2 V as shown in Fig. S3(c). Histogram shown in Fig. S3(b) represents all peak positions extracted from the d*I*/d*V* spectra of $CrBr_3$ taken at 77 K. Bins in the histogram are of width 0.1 V. Peak positions statistics is summarized in Table 1 in the main text.

Peaks labelled with numbers ("*1*" to "*4*") and letters ("*a*" to "*e*") are not observed in all these eight spectra since they are not in the same bias range or intensity range. Spectra taken with bias range of ± 0.8 V only show peaks "*1*" and "*a*"; spectra with bias range of ± 1 V show peaks "*a*", "*b*", "*1*" and "*2*"; spectra with bias range of ± 2 V show peaks "*a*-*c*", and "*1*-*3*". More peaks on the negative bias side ("*d*" and "*e*") and the positive bias side ("*3*" and "*4*") are observed in the spectra taken with bias range of ± 3 V, but the peaks "*a*-*c*", and "*1*-*2*" became too small to be observed. The histogram clearly indicates that the peak positions are highly repeatable.

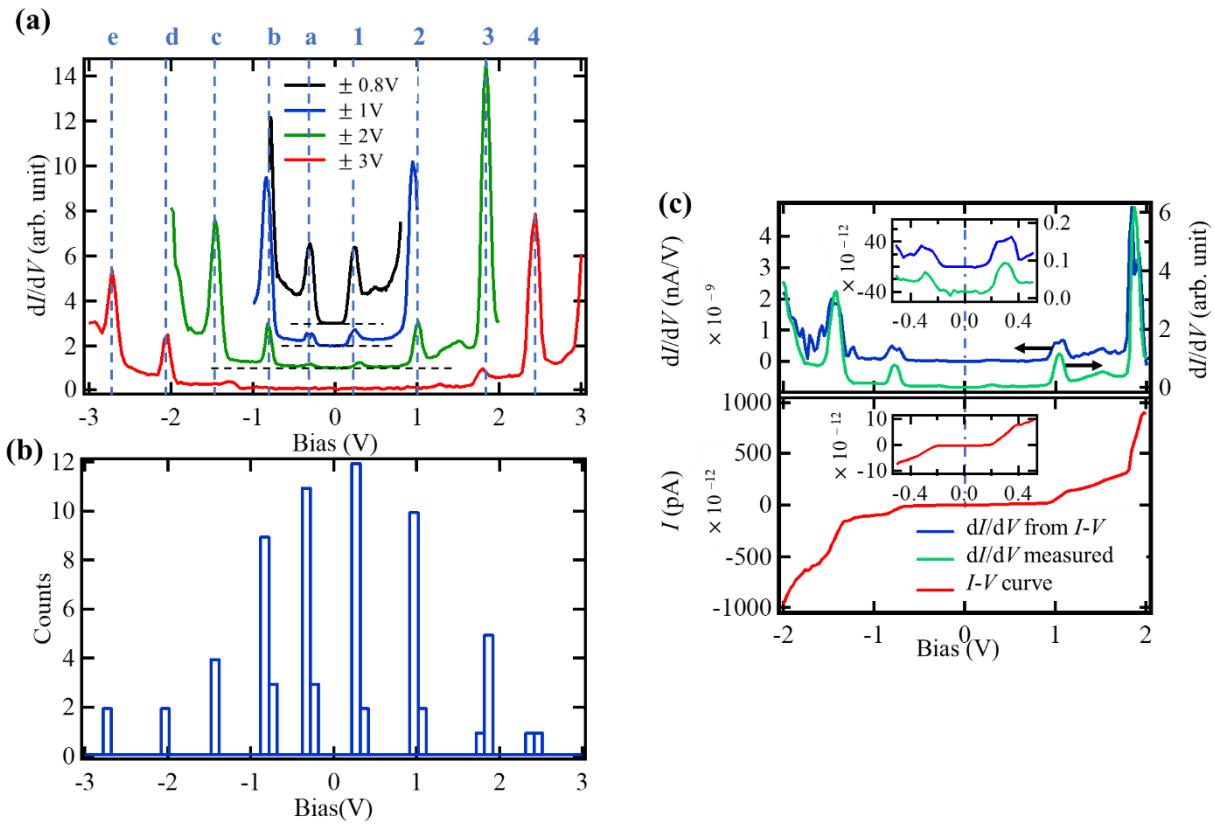

Figure S3. d*I*/d*V* spectra of bulk $CrBr_3$: (a) d*I*/d*V* spectra of $CrBr_3$ taken at 77 K with different bias ranges and sensitivity settings. **(b)** Histogram showing the peak positions in eight different d*I*/d*V* spectra of $CrBr_3$ taken at different bias range confirming the reproducible measurements. **(c)** Comparison between the numerically derived d*I*/d*V* spectrum (blue) from the measured *I*-*V* curve and the lock-in amplifier measured d*I*/d*V* spectrum (green). Insets are the magnified view to show features underlying in the bias range of ± 0.5 V. The blue curve is shifted upward for easy comparison. The measured *I*-*V* curve is shown in the bottom panel.

Table S1 shows all the possible combination of valence-conduction band peak pairs and their energy differences. These values are used to compare with the reported energies of the optical transitions, which are summarized in Table 2 in the main text.

Table S1. Energy differences between conduction-valence peak pairs. The peak symbols are defined in Figure 2(d).

Peak Pair	Energy Difference (eV)	Peak Pair	Energy Difference (eV)	Peak Pair	Energy Difference (eV)	Peak Pair	Energy Difference (eV)
1 - a	0.57 ± 0.04	**2 - a**	1.27 ± 0.05	**3 - a**	2.14 ± 0.04	**4 - a**	2.70 ± 0.08
1 - b	1.08 ± 0.06	**2 - b**	1.78 ± 0.07	**3 - b**	2.65 ± 0.06	**4 - b**	3.21 ± 0.09
1 - c	1.68 ± 0.04	**2 - c**	2.38 ± 0.05	**3 - c**	3.25 ± 0.04	**4 - c**	3.81 ± 0.08
1 - d	2.31 ± 0.04	**2 - d**	3.01 ± 0.05	**3 - d**	3.88 ± 0.04	**4 - d**	4.44 ± 0.08
1 - e	2.97 ± 0.04	**2 - e**	3.67 ± 0.05	**3 - e**	4.54 ± 0.04	**4 - e**	5.10 ± 0.08

S4. Comparing Individual and Area Averaged d*I*/d*V* Spectra: Figure S4 shows the comparison between the averaged (top panel) with the individual (bottom panel) d*I*/d*V* spectra. Overall, no obvious differences can be observed between them. The peak positions and the errors of the fitting extracted by Gaussian function fitting are shown in Table S2. Due to the high quality data, the fitting uncertainty of the peak position is extremely small. However, as described in the main text, there exist peak shifts among different measurements at the order of 0.1 V. This is clearly seen at peak "4" in the averaged curve. Since the averaged d*I*/d*V* spectrum cannot provide the peak shift deviation clearly, and the individual d*I*/d*V* spectra have very high signal-to-noise-ratio, we decided to analyze the individual d*I*/d*V* spectra, which can provide standard deviations among different peak positions, as summarized in Table 1 in the main text.

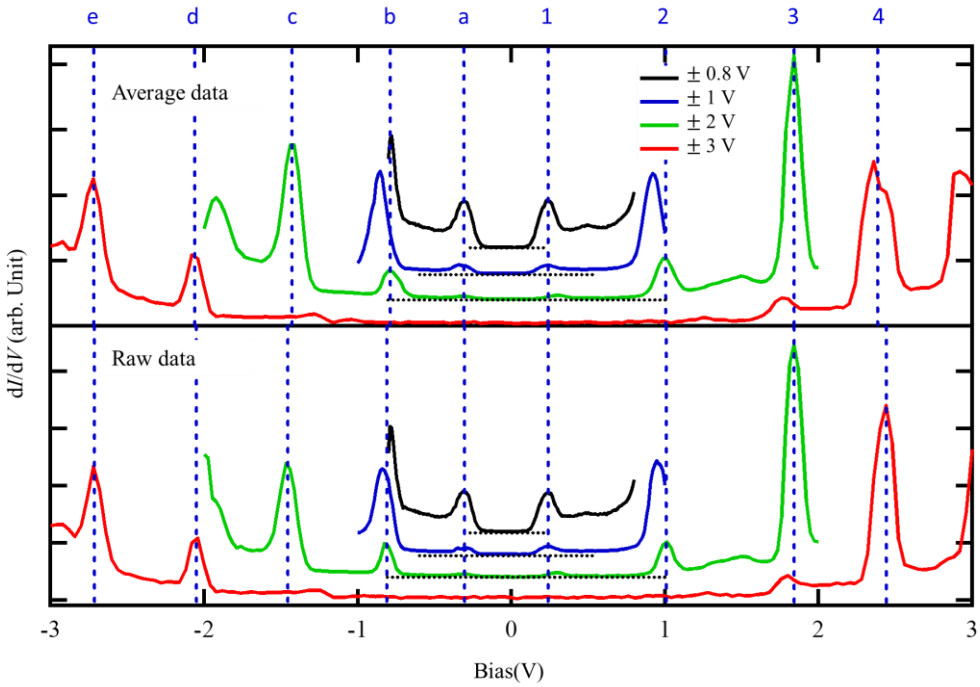

Figure S4. Averaged and Individual d*I*/d*V* Spectra: Top panel: averaged d*I*/d*V* spectrum; Bottom panel: individual d*I*/d*V* spectrum.

Table S2. Peak positions extracted from the averaged and individual d*I*/d*V* spectra shown in Figure S4.

Assigned peak symbols	**Peak positions (eV)**	
	Individual d*I*/d*V*	**Averaged d*I*/d*V***
4	2.428 ± 0.002	2.376 ± 0.005
3	1.839 ± 0.001	1.836 ± 0.001
2	1.007 ± 0.001	0.9986 ± 0.0004
1	0.232 ± 0.001	0.2340 ± 0.001
a	− 0.309 ± 0.001	− 0.307 ± 0.001
b	− 0.812 ± 0.001	− 0.782 ± 0.001
c	− 1.457 ± 0.001	− 1.428 ± 0.001
d	− 2.054 ± 0.001	− 2.062 ± 0.001
e	− 2.712 ± 0.002	− 2.723 ± 0.003